Symmetry restoration in mixed-spin paired heavy nuclei

Ermal Rrapaj, A. O. Macchiavelli, and Alexandros Gezerlis

Phys. Rev. C **99**, 014321 — Published 28 January 2019

DOI: 10.1103/PhysRevC.99.014321

Symmetry Restoration in Mixed-Spin Paired Heavy Nuclei

Ermal Rrapaj,[1] A. O. Macchiavelli,[2] and Alexandros Gezerlis[1]

[1]*Department of Physics, University of Guelph, Guelph, Ontario N1G 2W1, Canada*
[2]*Nuclear Science Division, Lawrence Berkeley National Laboratory, Berkeley, CA 94720, USA*

The nature of the nuclear pairing condensates in heavy nuclei, specifically neutron-proton (spin-triplet), versus identical-particle (spin-singlet) pairing has been an active area of research for quite some time. In this work, we probe three candidates that should display spin-triplet, spin-singlet, and mixed-spin pairing. Using theoretical approaches such as the gradient method and symmetry restoration techniques, we find the ground state of these nuclei in Hartree-Fock-Bogoliubov theory and compute ground-state to ground-state pair-transfer amplitudes to neighbouring isotopes while simultaneously projecting to specific particle number and nuclear spin values. We identify specific reactions for future experimental research that could shed light on spin-triplet and mixed-spin pairing.

I. INTRODUCTION

The presence of pairing in atomic nuclei has been established for more than five decades [1]. Extensive experimental data on nuclear properties: even-even excitation gaps, binding energy differences, moments of inertia, onset of deformation, two-nucleon transfer reactions, etc. can be explained by the presence of neutron-neutron (nn) and proton-proton (pp) Bardeen-Cooper-Schrieffer (BCS) like-pairing [2–4].

For most known nuclei, with neutron excess, the ground state consists of nn and pp ($j = 0$, $t = 1$) pairs coupled to angular momentum $J = 0$. For nuclei with comparable number of neutrons and protons, the nucleons near the Fermi surface should occupy identical orbitals and np pairing should be present. Due to the Pauli exclusion principle, isospin-singlet/isoscalar ($t = 0$) is associated with spin-triplet ($s = 1$) pairing, and vice-versa.

The elusive spin-triplet pairing in nuclei has been both an experimental and theoretical puzzle over the decades [5]. Charge independence of the nuclear force should lead to both ($j = 0, t = 1$) nn and pp pairing on equal footing with ($j = 0, t = 1$) np pairing for nuclei with $N \approx Z$. In addition, the existence of the deuteron as a $J^\pi = 1^+$ bound state and low energy scattering data [6] indicate that the strength of the interaction is stronger in the isocalar channel in comparison to nucleons coupled to isospin 1. The natural conclusion from this observation is the expectation to find isospin-singlet, spin-triplet pairing in nuclei, in the form of a *quasi-deuteron* condensate.

Neutron-proton pair correlations have been studied by analyzing the results of large-scale shell model calculations [7–15]. The spin-orbit interaction tends to suppress spin-triplet pairing [16, 17], and nuclear deformation also plays a competitive role and therefore needs to be treated in detail [18]. In the case of $N \approx Z$, and large atomic number, if one assumes spherical symmetry, it reasonably to expect this type of pairing.

However, in finite systems, pairing can be difficult to define, and many proxies have been used in literatue [7–9, 11, 12]. The energy competition between the spin-singlet and spin-triplet states has also been studied [49]. The most direct measure would be to calculate the pair-transfer reaction probabilities [3, 4] and here we calculate the pair-transfer amplitude in the framework of Hartree-Fock-Bogoliubov (HFB) theory.

The Hartree-Fock-Bogoliubov approach is a versatile tool that can describe a large number of many-nucleon problems where pairing is important [19]. The basics of the HFB formalism are covered in section II. Pairing studies in nuclear physics have included an isovector pairing field, an isoscalar pairing field, and coexisting ($t = 0, 1$) pairing fields for $N = Z$, as well as general nucleon numbers [20–28]. More recently, a mixed-spin pairing ground state was found to be energetically favourable, in the context of HFB theory, for the case of heavy nuclei [29, 30] (see also Ref. [31]).

In this work, we focus our attention to the $A \geq 130$ region close to the proton dripline. In Ref. [29] many candidates where $t = 0$ pairing could be present were found in this area. While we are aware that transfer reaction studies on these nuclei are currently not possible, this part of the nuclear chart could be accessible to experimental research via selective studies of fusion-evaporation reactions. Thus our findings, based on the analysis of two-nucleon overlaps, can guide the experimental program to those nuclei where the presence of spin-triplet pairing phase near the ground state is more probable.

The first step, then, is finding the ground state for a given nucleus. In practice, particle number and nuclear spin are not conserved, and need to be restored. Employing the gradient method developed in Ref. [32] we find the minimal energy wave-function. This method allows one to constrain the expectation value of particle number and the amplitudes of various pairing channels. We do so to explore how various constraints impact not only the energy of the ground state but also its composition in terms of eigenstates of the symmetry operators under consideration.

Symmetry restoration can be a non-trivial task. In the past, various formulae based on determinants have been used, which suffer from a sign ambiguity [33]; and various approximations to overcome it have been employed

[34–37]. Ambiguity-free formulations have been recently developed [38–40]. We make use of the expressions derived in Ref. [38], which do not have the shortcoming mentioned.

As found in Refs. [29, 30], there are nuclei where one type of pairing dominates, like spin-triplet in $^{132}_{66}$Dy, or spin-singlet in $^{132}_{60}$Nd. Also nuclei with coexistence of both types are present in the nuclear chart, like the so called mixed-spin pairing in $^{132}_{64}$Gd. The distributions of the states of good quantum numbers for the ground state of each of these three nuclei are analyzed in subsections III A, III B, and III C.

Another area of investigation is how pair-transfer cross-sections (probabilities) compare in ground-state to ground-state transitions [41], an observable that could be considered as the *smoking gun* to disentangle the two effects. We compute various transitions from the neighbouring isotopes of the three nuclei mentioned, while simultaneously carrying out a symmetry projection.

In this paper, our goal is two-fold: i) To confirm the nature of the ground state condensates survives after projection, and ii) For future studies, to find the most promising pair-transfer reactions for each case. A detailed discussion can be found in section IV, and we draw our conclusions in the last section.

II. THE HFB FORMALISM

The HFB theory is based upon a variational principle for the energy of the ground state of the system. The many body wave-function is varied in the space of Slater determinants of quasi-particles defined by the Bogoliubov transformation. The 'effective' Hamiltonian in this theory consists of one body and two body operators, which we write in second quantization language, in terms of spin half particle operators as

$$\hat{H} = \sum_{i,j} t_{ij} c_i^\dagger c_j + \frac{1}{4} \sum_{i,j,k,l} \overline{v}_{ijkl} c_i^\dagger c_j^\dagger c_l c_k \tag{1}$$

The one body potential used in this work is of Wood-Saxon shape including contributions from spin-orbit interactions,

$$\begin{aligned} v(\boldsymbol{r}) =& V_{WS} f(r) - (\boldsymbol{L}\cdot\boldsymbol{S}) \frac{V_{SO}}{r}\frac{df}{dr} \\ f(r) =& [1+e^{(r-R)/a}]^{-1} \end{aligned} \tag{2}$$

and the two body interaction is a contact term for each of the pairing channels given in table I,

$$\begin{aligned} V(\boldsymbol{r}_1,\boldsymbol{r}_2) =& \sum_{\alpha}^{6} v_\alpha P_{L=0} P_\alpha \delta^3(\boldsymbol{r}_1-\boldsymbol{r}_2) \\ =& \frac{1}{4}\bigg(3v_t + v_s + (v_t - v_s)\boldsymbol{\sigma}_1\cdot\boldsymbol{\sigma}_2\bigg) \\ & \times \delta^3(\boldsymbol{r}_1-\boldsymbol{r}_2) P_{L=0} \end{aligned} \tag{3}$$

The numerical values for the parameters v_s and v_t are 300 MeV and 450 MeV respectively, taken from Ref. [30]. The Bogoliubov transformation from particle to quasi-particle space is defined as follows,

$$\begin{pmatrix} \boldsymbol{\beta} \\ \boldsymbol{\beta}^\dagger \end{pmatrix} = \begin{pmatrix} U^\dagger & V^\dagger \\ V^T & U^T \end{pmatrix} \begin{pmatrix} \boldsymbol{c} \\ \boldsymbol{c}^\dagger \end{pmatrix} \tag{4}$$

As a result, the Hamiltonian can be expressed in the new basis,

$$\hat{H} = H^{00} + \boldsymbol{\beta}^\dagger H^{11} \boldsymbol{\beta} + \frac{1}{2}\boldsymbol{\beta}^\dagger H^{20} \boldsymbol{\beta}^\dagger + ... \tag{5}$$

where the superscripts count the number of creation and annihilation operators of quasi-particles. A more detailed explanation of the various terms appearing in Eq. (5) can be found in Ref. [30].

A. General Features of the ground state

The ground state wave-function used in this work is defined as follows,

$$|\Phi\rangle = \mathrm{pf}(U^\dagger V^*) \, \exp\left[\frac{1}{2}(VU^{-1})^*{}_{ij} c_i^\dagger c_j^\dagger\right] |0\rangle \tag{6}$$

where pf() is the Pfaffian of the matrix, and $|0\rangle$ is the reference vacuum state. The three main isotopes investigated here share the same reference vacuum state, and the same quasi-particle basis which technically is infinite. Different isotopes occupy different sub-spaces and when their overlap is calculated, an augmented subspace which encompasses both nuclei is used [42]. The minimization of the energy is performed through the gradient method described in Ref. [32] subject to neutron and proton number constraints. In addition, the various nucleon pairing channels can be constrained [30], and the constrained Hamiltonian is,

$$\hat{H}_c = \hat{H} - \sum_\alpha \lambda_\alpha \hat{Q}_\alpha \tag{7}$$

The parameters λ_α are analogous to Lagrange multipliers and the operators Q_α are particle number, pairing amplitudes etc. In this sense, this formulation employs the grand canonical ensemble.

As already mentioned in the introduction, the three representative isotopes analyzed here are $^{132}_{60}$Nd, $^{132}_{64}$Gd , and $^{132}_{66}$Dy, taken from Ref. [30]. While there is a distribution of eigenstates with specific quantum numbers in the ground state found, we enforce this distribution to be highly peaked at the target isotope.

All the various possible pairing channels are given in table I. In table II we report the correlation energy, the energy difference between the unpaired ground state and the one without any suppression of pairing, found for each isotope subject to pairing constraints. Since the

	1	2	3	4	5	6
$(S,\ S_z)$	(0, 0)	(0, 0)	(0, 0)	(1, 1)	(1, 0)	(1,-1)
$(T,\ T_z)$	(1, 1)	(1, 0)	(1, -1)	(0, 0)	(0, 0)	(0, 0)

TABLE I. The 6 spin-isospin pairing channels

	$^{132}_{66}$Dy	$^{132}_{64}$Gd	$^{132}_{60}$Nd
	(spin-triplet)	(mixed-spin)	(spin-singlet)
No Constraint	11.315	7.478	8.037
No $S=0$	11.315	6.299	1.630
No $S=1$	4.853	4.630	8.035

TABLE II. The correlation energy E_{corr}[MeV]. This quantity is defined as the difference in HFB ground state binding energy between the unpaired nucleus and the one subject to pairing constraints (or completely unconstrained).

present calculations are at mean field level, the results are to be understood more as a qualitative rather than quantitative representation of the 'physical' ground state. As can be seen from table II, the unconstrained ground state and the one found by removing spin-singlet pairing are nearly degenerate in energy for $^{132}_{66}$Dy. This is an indication of this nucleus exhibiting mainly spin-triplet pairing. The situation in the case of $^{132}_{64}$Gd is quite different. Neither pairing channel is suppressed in the ground state, and both pair constrained states have very similar values of correlation energy. We, thus, can expect $^{132}_{64}$Gd to be of spin-mixed pairing nature. The last isotope, $^{132}_{60}$Nd, is analogous to $^{132}_{66}$Dy, but for spin-singlet pairing. Note that when we refer to a nucleus as exhibiting, say, spin-singlet pairing, we merely mean that the channel is dominant (not that it's the only one present).

B. The Eigenbasis

The basis chosen is block diagonal in orbital angular momentum $\hat{L}$ (multiple l values are present), and diagonal in isospin $\hat{T}$, and spin $\hat{S}$. The symmetries we are studying are particle number $\hat{A}$, more specifically neutron and proton number, and nuclear spin ($\hat{\boldsymbol{J}} = \hat{\boldsymbol{L}} + \hat{\boldsymbol{S}}$). The respective operators are represented by matrices in this basis,

$$\begin{aligned}\hat{A}^{(LTS)} &= \mathbb{I}_{N_L} \otimes \mathbb{I}_2 \otimes \mathbb{I}_2 \\ \hat{T}^{(LTS)} &= \mathbb{I}_{N_L} \otimes J_{1/2} \otimes \mathbb{I}_2 \\ \hat{J}_z^{(LTS)} &= \{\oplus J_{L_i}\} \otimes \mathbb{I}_2 \otimes \mathbb{I}_2 + \mathbb{I}_{N_L} \otimes \mathbb{I}_2 \otimes J_{1/2} \\ N_L &= \sum_i (2L_i + 1)\end{aligned} \tag{8}$$

where J_D is the angular momentum operator in the irreducible diagonal representation in which D is the maximal eigenvalue of $\hat{J}_z$ [43]. $\mathbb{I}_{N_L}$ is the N_L dimensional identity matrix.

III. SYMMETRY RESTORATION

Following previous work, we find the ground state through energy minimization and then perform symmetry projection, also called projection after variation (PAV) [41, 44, 45]. The energy minimization procedure does not respect either $\hat{A}$ or $\hat{J}$ conservation, and these symmetries are restored by projecting out the eigenstate composition of the wave-function found.

The probability for a quantum number K to be present in the wave-function $|\Phi\rangle$ is given by the formula,

$$\langle\Phi|\hat{P}^K|\Phi\rangle = \frac{d_K}{\Omega_0}\int d\Omega\ P^K_{II}(\Omega)\ \langle\Phi|\mathcal{P}(\Omega)|\Phi'\rangle \tag{9}$$

where $P^K_{II}(\Omega)$ is a diagonal matrix element of the symmetry group P in representation of dimensionality d_K, and Ω_0 is the volume integral of the group. The overlap $\langle\Phi|\mathcal{P}(\Omega)|\Phi'\rangle$ is calculated based on the expressions from Ref. [38]. The numerical implementation of the Pfaffian is based on the Parlett-Reid algorithm as shown in Ref. [46].

A. Particle number projection

In the case of simultaneous projection of proton and neutron number, the projection operator is,

$$\begin{aligned}\hat{P}^{(LTS)}_{NZ}(N_0, Z_0) &= \int_0^{2\pi}\frac{d\varphi_N}{2\pi}e^{-iN_0\varphi_N}\int_0^{2\pi}\frac{d\varphi_Z}{2\pi}e^{-iZ_0\varphi_Z} \\ &\quad\times\ e^{iR(\varphi_N,\varphi_Z)} \\ R(\varphi_N,\varphi_Z) &= \mathbb{I}_{N_L}\otimes\begin{pmatrix}\varphi_N & 0\\ 0 & \varphi_Z\end{pmatrix}\otimes\mathbb{I}_2\end{aligned} \tag{10}$$

As the plot in Fig. 1 shows, the presence of only spin-triplet pairing forces the probability distributions for protons and neutrons to be strongly coupled (the distribution is perpendicular to the $A = 132$ line). If only spin-singlet is present, the distributions are de-coupled and there is a checker-board pattern centered at the target isotope. Mixed-spin pairing is a hybrid of the two previous configurations. Note that for each of the three nuclei under study we see contributions coming from several even-even and odd-odd nuclides (this is true also for $^{132}_{60}$Nd, where the odd-odd contributions are tiny but their cumulative contribution to $I_0 = 1$ is noticeable as shown in the following sections).

To have a better understanding of the pattern observed, it is instructive to perform symmetry restoration on the mixed-spin isotope, by constraining one type of pairing at a time, to see how the ground state configuration looks in terms of neutron and proton number distributions. As displayed in Fig. 2, the pattern found in Fig. 1 persists; spin triplet pairing symmetrizes the distributions while spin singlet completely decouples them.

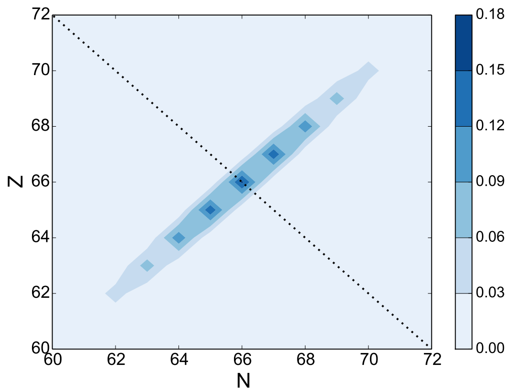

(a) $^{132}_{66}$Dy

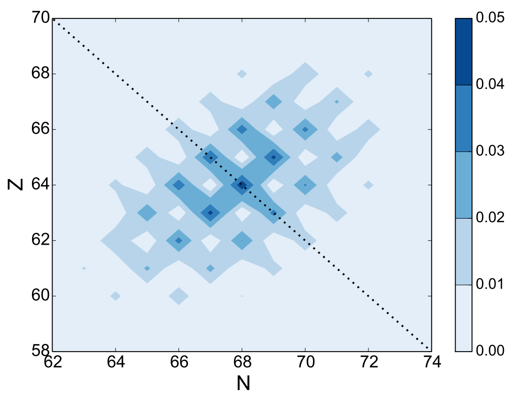

(b) $^{132}_{64}$Gd

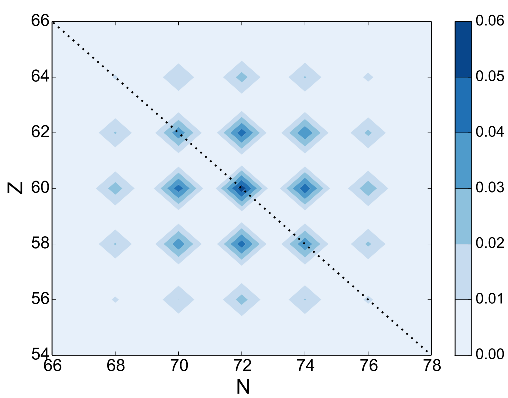

(c) $^{132}_{60}$Nd

FIG. 1. Two dimensional probability distributions, Eq. (9) with the projection operator in Eq. (10). Dotted line represents $A = 132$.

As a check, we have carried out further calculations, where we remove spin-singlet pairing from the ground state of $^{132}_{66}$Dy: there was no significant change in the particle number distribution. The same turned out to be the case when removing spin-triplet pairing for $^{132}_{60}$Nd. In order to avoid any confusion when reading our two-dimensional distribution plots, we emphasize here that projection to only integer particle number was performed, since N and Z are treated as integers throughout this work.

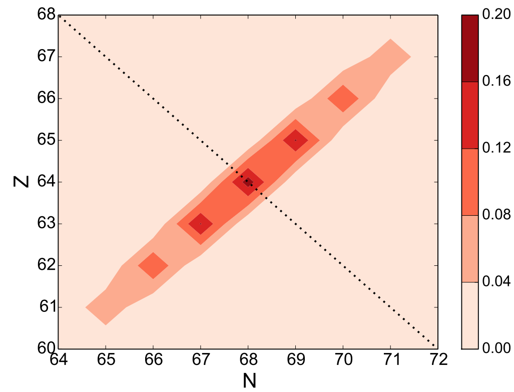

(a) No spin-singlet pairing

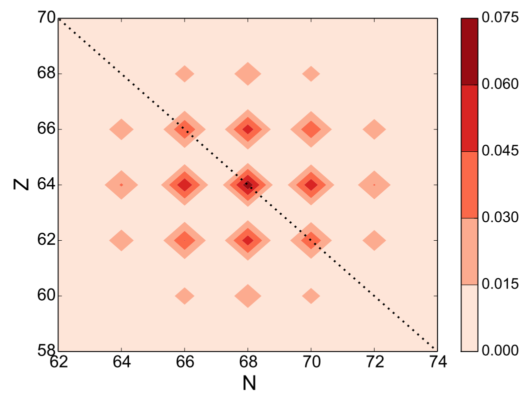

(b) No spin-triplet pairing

FIG. 2. Two dimensional probability distribution for $^{132}_{64}$Gd subject to pairing constraints. Dotted line represents $A = 132$.

B. Angular momentum projection (nuclear spin)

The rotational group is parametrized in terms of the three Euler angles $\Omega = (\alpha, \beta, \gamma)$ and the symmetry group under consideration is SU(2). The respective expression for $\hat{J}$ projection is [19],

$$\begin{aligned}\hat{P}_J^{(LTS)}(I_0, m', m) = \frac{2I_0+1}{8\pi^2} \int_0^{2\pi} d\alpha \int_0^{\pi} d\beta \sin(\beta) \\ \times \int_0^{2\pi} d\gamma e^{i(m'\alpha + m\gamma)} d^{(I_0)}_{m',m}(\beta) e^{i\alpha \hat{J}_z^{(LTS)}} \\ \times \quad e^{i\beta \hat{J}_y^{(LTS)}} e^{i\gamma \hat{J}_z^{(LTS)}}\end{aligned} \tag{11}$$

where $d^{(I_0)}_{m',m}(\beta) = \langle I_0, m' | \exp[i\beta \hat{J}_y] | I_0, m\rangle$ is the Wigner matrix representing the rotation matrix element around the y-axis in the $\hat{J}_z$ basis [47]. We used a slight modification of Eq. (11), where the range of integration for γ is twice the full rotation, and the projection operator

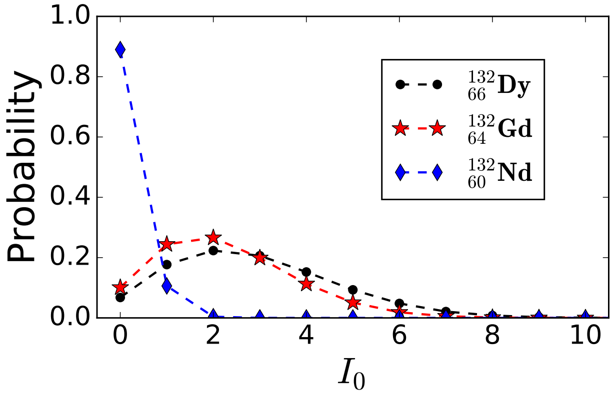

FIG. 3. I_0 probability distribution, Eq. (9) with the projection operator in Eq. (11), for $^{132}_{66}$Dy (black–circle), $^{132}_{64}$Gd (red–star), and $^{132}_{60}$Nd (blue–diamond).

was normalized accordingly. The reason for this change is to allow for the simultaneous projection of both half and full angular momentum values. If the number of quasi-particles is even, only integer values of I_0 are to be expected, but for odd number nuclei, spin half values might be present.

Fig. 3 depicts the I_0 probability distribution for all three isotopes. In the case of spin-singlet pairing ($^{132}_{60}$Nd) $I_0 = 0$ is the dominant state; and in the case of spin-triplet pairing ($^{132}_{66}$Dy), there is a spread peaked at low values of I_0. Interestingly, the mixed-spin paired isotope resembles more the spin-triplet distribution. The probability distributions for I_0 subject to all the pairing constraints for the mixed-spin pairing isotope are depicted in Fig. 4. A rather intriguing pattern emerges from this figure; when only spin-singlet pairing is present, $I_0 = 0$ is the only value present, and when only spin-triplet pairing is present, there is a wide spread of possible I_0 values.

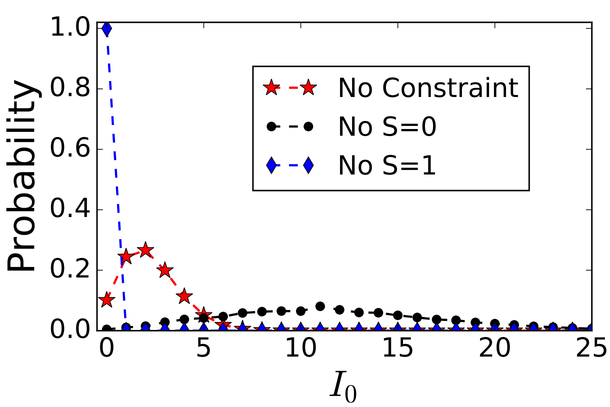

FIG. 4. I_0 probability distribution, as in Fig. 3, for $^{132}_{64}$Gd subject to no constraint (red–star), no spin-singlet (black–circle), and no spin-triplet (blue–diamond) pairing.

C. Particle number and angular momentum

In order to identify what fraction of the ground state has the 'right' quantum numbers (N_0, Z_0, I_0), a simultaneous projection is required:

$$\hat{P}^{(LTS)}_{NZJ}(N_0, Z_0, I_0) = \hat{P}^{(LTS)}_{NZ}(N_0, Z_0) \sum_{m=-I_0}^{I_0} \hat{P}^{(LTS)}_{J}(I_0, m, m) \tag{12}$$

In Fig. 5 we plot the particle number probability distributions for the three isotopes after we have projected to

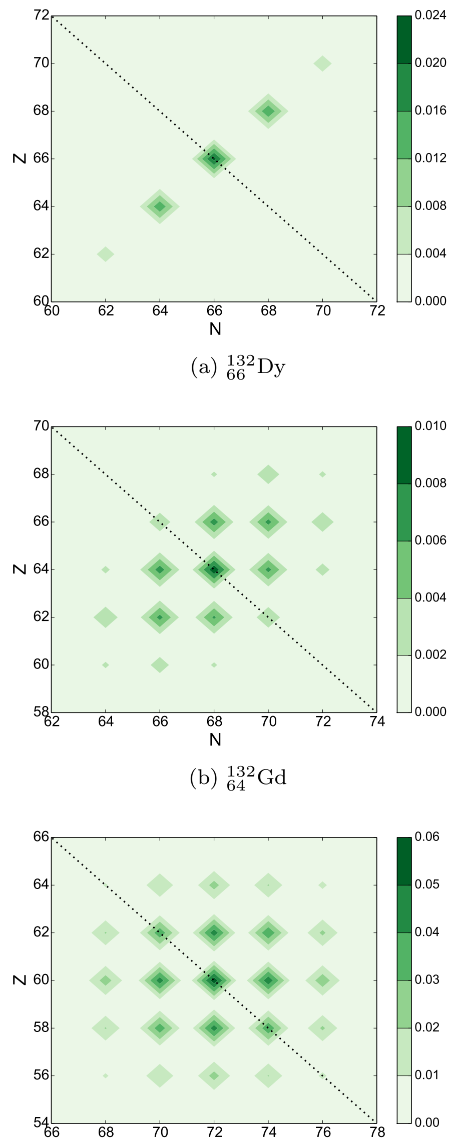

(a) $^{132}_{66}$Dy

(b) $^{132}_{64}$Gd

(c) $^{132}_{60}$Nd

FIG. 5. Two dimensional probability distributions for the three isotopes for $I_0 = 0$, Eq. (9) with the projection operator in Eq. (12), without any constraint on pairing. Dotted line represents $A = 132$.

$I_0 = 0$ chosen to represent the ground state. As can be seen from the plot, for $^{132}_{66}$Dy and $^{132}_{64}$Gd there is rather a sparse probability distribution which agrees with the result of Fig. 3 which shows that $I_0 = 0$ is a very small part of the wave-function. The distribution for $^{132}_{60}$Nd is almost the same as in Fig. 1, as 90 % of the wave-function has $I_0 = 0$. A rather interesting feature emerges from this Figure; there are no odd-odd nuclei making up the distribution for $I_0 = 0$, despite the fact that they were present present in each of the full HFB ground states (Fig. 1). To further understand this situation, we also carried out separate calculations, projecting to $I_0 = 1$ and examining the particle number distribution for each isotope. The result of the projection is depicted in Fig. 6. We (correspondingly) find that only odd-odd nuclei make up the $I_0 = 1$ distributions.

Fig. 7 depicts the I_0 distribution for each isotope after the neutron and proton particle numbers have been projected to the target values. By comparing with Fig. 3, we notice that $^{132}_{60}$Nd has only $I_0 = 0$ for the target particle numbers, while the 2 other isotopes have the same qualitative shape as in the previous plot.

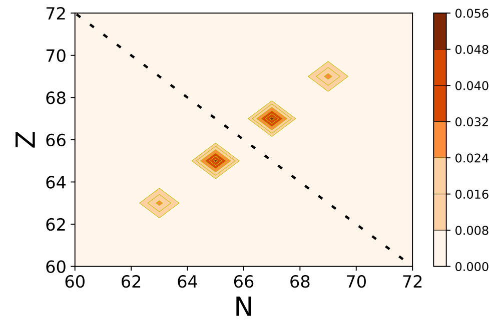

(a) $^{132}_{66}$Dy

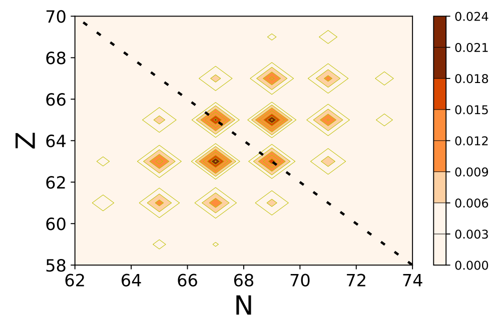

(b) $^{132}_{64}$Gd

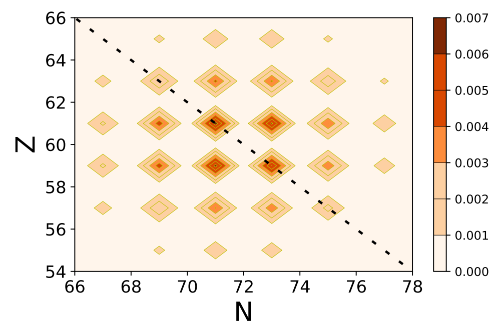

(c) $^{132}_{60}$Nd

FIG. 6. Two dimensional probability distributions for the three isotopes for $I_0 = 1$, Eq. (9) with the projection operator in Eq. (12), without any constraint on pairing. Dotted line represents $A = 132$.

IV. PAIR TRANSFER

A. Wave-function overlap and particle creation operators

Apart from analyzing the eigen-composition of the HFB ground state, we are also interested in applying symmetry restoration to ground-state to ground-state pair-transfer reactions. While this overlap has been treated extensively in various approximations [41] [48], our focus here is in finding the most probable pair-transfer reaction for nuclei where spin-triplet pairing could be present. In particular, we study all the overlaps between the 3 nuclei under study and the neighbouring isotopes that can be reached by the addition of 2 nucleons. Instead of assuming that the initial and final nuclei are the same, as is sometimes done, we explicitly include the appropriate HFB nuclei. The expressions for the overlap with inclusion of addition/removal of particles are derived from Ref. [38],

$$\langle\Phi|\mathcal{P}(\Omega)c^\dagger_{q_1}c^\dagger_{q_2}|\Phi'\rangle = \frac{(-1)^{n(n-1)/2}}{\langle\Phi|\Phi'\rangle} \times \ \mathrm{pf}\begin{pmatrix} V^tU & V^tP^*q^t & V^tP^*V'^* \\ -qP^\dagger V & 0 & 0 \\ -V'^\dagger P^\dagger\, V & 0 & U'^\dagger V'^* \end{pmatrix} \tag{13}$$

where the$(U,\ V)$ matrices, describing the wave-function in Eq. (6), have dimensions $(2n,\ 2n)$, q is a $(2, 2n)$ matrix whose rows are the vector representations of the particles creation operators in the wave-function basis. Note that, $\langle\Phi|\mathcal{P}(\Omega)c^\dagger_{q_1}c^\dagger_{q_2}|\Phi'\rangle = \langle\Phi'|c_{q_1}c_{q_2}\mathcal{P}^\dagger(\Omega)|\Phi\rangle^*$, so the expression provided can be used for both pair addition or removal.

B. Creation-operator representation

The projection operator and its representation has been dealt with in section II B. Here, we describe how to construct the creation operators of specific quantum numbers (I_0, m_I, m_T).

We start with a basis diagonal in $(\hat{\boldsymbol{J}}^2\ \hat{J}_z)$, where we assume that also $(\hat{J}_x,\ \hat{J}_y)$ are in their standard representation [43]. A creation operator of specific $(I_0,\ m_I)$ quantum numbers is represented by $\boldsymbol{e}_i$, the i^{th} column of

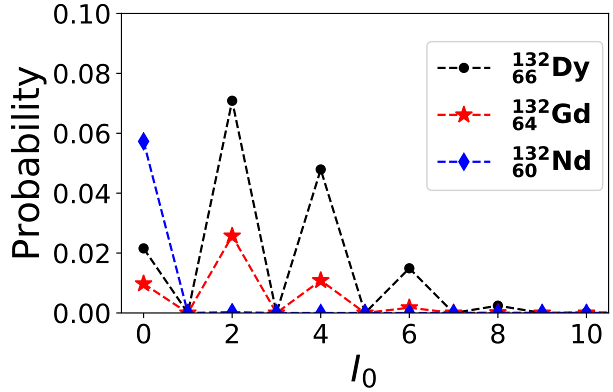

FIG. 7. I_0 probability distribution for $^{132}_{66}$Dy (black–circle), $^{132}_{64}$Gd (red–star), and $^{132}_{60}$Nd (blue–diamond). Each isotope has been projected to the respective target neutron and proton numbers.

the identity matrix $\mathbb{I}$, which is also an eigenvector of $\hat{J}_z$,

$$\boldsymbol{q} = \boldsymbol{e}_i,\ \hat{\boldsymbol{J}}^2\boldsymbol{e}_i = I_0(I_0+1)\boldsymbol{e}_i,\ \hat{J}_z\boldsymbol{e}_i = m_I\boldsymbol{e}_i \tag{14}$$

Given that $(\hat{\boldsymbol{J}}^2,\ \hat{J}_z)$ commute, the transformation from the $(\hat{\boldsymbol{L}}, \hat{\boldsymbol{S}})$ basis to the $\hat{J}_z$ basis is achieved through constructing a matrix pencil [50]. An additional similarity transformation which sets $(\hat{J}_x,\ \hat{J}_y)$ in their standard forms and leaves $(\hat{\boldsymbol{J}}^2,\ \hat{J}_z)$ invariant is required. Let us denote the successive application of these two transformations as Q:

$$J_z^{(LS)} = Q\ J_z^{(j,m_j)}\ Q^\dagger \tag{15}$$

And, in the basis of the HFB wavefunction,

$$\{\oplus J_{L_i}\} \otimes \mathbb{I}_2 + \mathbb{I}_{N_L} \otimes J_{1/2} = J_z^{(LS)} \tag{16}$$

The order of the operators in the HFB basis is orbital angular momentum — isospin — spin (LTS), and we need to have isospin — orbital angular momentum — spin (TLS). The order reshuffling can be performed with the use of permutation matrices $S_{p,r} = \sum_{i=1}^{p} \boldsymbol{e}_i^t \otimes \mathbb{I}_r \otimes \boldsymbol{e}_i$ [51]. The main property of these matrices is to change the order of a Kronecker product. The complete reordering between the two bases is performed,

$$\begin{aligned}J_z^{(LTS)} =& \{\oplus J_{L_i}\} \otimes \mathbb{I}_2 \otimes \mathbb{I}_2 + \mathbb{I}_{N_L} \otimes \mathbb{I}_2 \otimes J_{1/2}\\ =& S_{N_L,4}\left[\mathbb{I}_2 \otimes \left(\mathbb{I}_2 \otimes \{\oplus J_{L_i}\} + J_{1/2} \otimes \mathbb{I}_{N_L}\right)\right] S_{N_L,4}^t\\ =& S_{N_L,4}\left[\mathbb{I}_2 \otimes \left(S_{2,N_L}\ J_z^{(LS)}\ S_{2,N_L}^t\right)\right] S_{N_L,4}^t\end{aligned} \tag{17}$$

As a careful reader might notice, two successive permutations are performed, the first one is $(LTS \longrightarrow TSL)$ and the second one is $(TSL \longrightarrow TLS)$. This leads us to connect the basis used to find the HFB ground state with a basis in which particle creation/ annihilation operators with specific nuclear spin quantum numbers can be easily expressed in matrix notation.

$$\boldsymbol{q}^{(\text{HFB basis})} = S_{N_L,4}\left[\mathbb{I}_2 \otimes \left(S_{2,N_L}\ Q\ \boldsymbol{e}_i\ Q^\dagger\ S_{2,N_L}^t\right)\right] S_{N_L,4}^t \tag{18}$$

C. Pair transfer amplitude

In order to estimate which pair transfer reaction is more probable, for each of the three nuclei studied so far, we define the pair-transfer amplitude rate as follows,

$$\begin{aligned}&\mathcal{A}^{(J_p)}_{\Phi_i,\Phi_f}(I_i, I_f) = \left|\frac{\langle\Phi_f|\hat{\mathscr{P}}(I_f, J_p)|\Phi_i\rangle}{\mathcal{N}_i\mathcal{N}_f}\right|\\ &\hat{\mathscr{P}}(I_f, J_p) = \sum_{m_{j_p}=-J_p}^{J_p} \hat{P}_J(I_f)\hat{c}^{\dagger(J_p,-m_{j_p})}\hat{c}^{\dagger(J_p,m_{j_p})}\\ &\mathcal{N}_i = \sqrt{\langle\Phi_i|\hat{P}_J(I_i)|\Phi_i\rangle};\ \mathcal{N}_f = \sqrt{\langle\Phi_f|\hat{P}_J(I_f)|\Phi_f\rangle}\end{aligned} \tag{19}$$

where (I_i, I_f) are the nuclear spin values of the ground states of the two nuclei. For isotopes with even number of neutrons and protons, we assume this value to be $I_i = 0$, $I_f = 0$ and for isotopes with odd number of neutrons and odd number of protons we take it to be $I_i = 1$. J_p refers to the total angular momentum of each particle in the pair, as explained in detail in IV B. We assume that both particles in the pair have the same angular momentum and opposite projection in the $\hat{z}$ direction. The symmetry projection operator acts to the left on the final state, which has been studied in detail in the previous sections.

We create single-particle states with quantum numbers $(n,\ l,\ J_p,\ m_{j_p})$, where l takes the values $(0,\ 2,\ 4,\ 5)$ (with n respectively $(0,\ 1,\ 2,\ 3)$) [30, 31]. For instance, if $J_p = 1/2$, the orbital angular momentum is $l = 0$ and $n = 0$. In what follows, we quote the total angular momentum value J_p as shorthand.

In Eq. (19) we did not include the simultaneous (N, Z, J) projection since it is computationally expensive, but we computed it for $(N, Z, J_p = 1/2)$ and the qualitative trends do not change.

There are various definitions of the transfer amplitude in literature [41], and given that the wave-function we use is not normalized to 1, we need to divide by the individual norms of initial and final nuclei. In addition, we are interested only in the fraction of the wave-function with the right ground state quantum numbers, so we normalize by the symmetry projected initial and final states.

Let us turn to a detailed discussion of Fig. 8. For $^{132}_{66}$Dy (panel a), the presence of spin-triplet pairing is in agreement with the addition of an np pair to the lighter isotopes being highly more likely than that of nn or pp pairs (which have equal transfer amplitudes). Thus, this is an

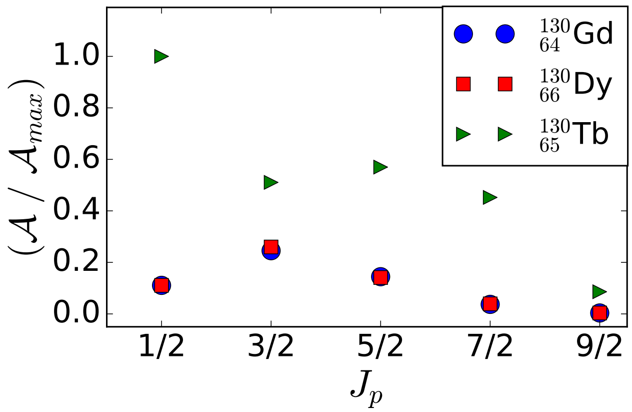

(a) Final isotope is $^{132}_{66}$Dy.

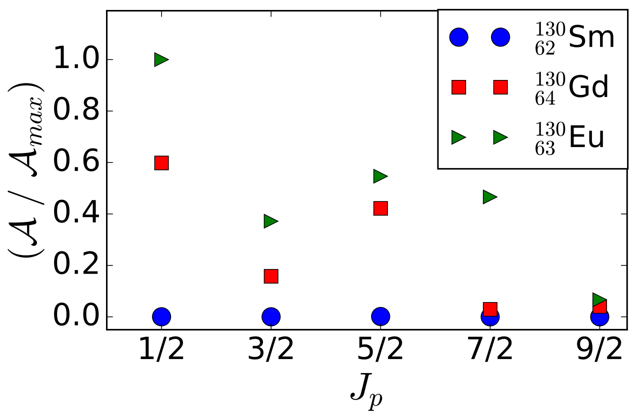

(b) Final isotope is $^{132}_{64}$Gd.

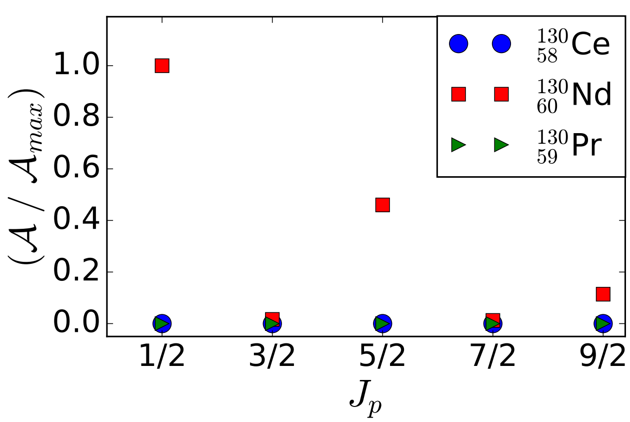

(c) Final isotope is $^{132}_{60}$Nd.

FIG. 8. Transfer amplitudes for pair addition processes. Blue circles correspond to pp transfer; red squares correspond to nn transfer, and green triangles correspond to np pair transfer.

additional piece of evidence on spin-triplet np pairing, since $^{130}_{65}$Tb→ $^{132}_{66}$Dy is the most likely reaction to occur. Since $^{132}_{66}$Dy is an $N = Z$ nucleus, if the np pairing was spin-singlet in nature, then the np pair transfer would have had the same amplitude as nn and pp pairs. Now turn to $^{132}_{64}$Gd (panel b): the situation is rather different, since there are more neutrons than protons. Since here nn and np transfer ampitudes are both non-zero, we see the presence of both spin-triplet and spin-singlet pairing. As it so happens, the spin-triplet pairing is responsible for the np amplitude being (somewhat) larger than the nn one. Finally, in $^{132}_{60}$Nd (panel c) where the excess of neutrons is sizable, the situation is reversed. We do not find any significant amplitude for np or pp pairs: this nucleus is characterized by spin-singlet pairing, with the most likely reaction being $^{130}_{60}$Nd→ $^{132}_{60}$Nd.

V. CONCLUSIONS

Symmetry restoration allows us to discern the particle number and nuclear spin eigenstate composition of the ground state wave-function found in HFB theory. By mapping out the probability distributions for each of these quantities for three isotopes, $^{132}_{66}$Dy, $^{132}_{64}$Gd, and $^{132}_{60}$Nd we were able to study how different types of spin pairings shape the eigen composition of the ground state. We were able to find specific patterns in the probability distributions that can be used as theoretical qualitative indications of spin-triplet, spin-singlet or mixed-spin pairing. In the case of spin-triplet pairing, the proton and neutron number distributions seem rather symmetric. In the spin-singlet case there is checkered pattern, and the mixed-spin pairing is in between.

The second part of this work focuses on calculating ground-state to ground-state pair-transfer amplitudes in order to find the most likely candidate reactions for probing spin-triplet and mixed-spin pairing in heavy nuclei. We find $^{130}_{65}$Tb→ $^{132}_{66}$Dy to be very likely, in good agreement with the spin-triplet nature of Dy. Similarly, $^{130}_{60}$Nd→ $^{132}_{60}$Nd is the most probable transition, which is another indication of spin-singlet pairing in this nucleus. The mixed-spin pairing case is more intricate, $^{130}_{63}$Eu→ $^{132}_{64}$Gd is the dominant reaction, which is an indication of spin-triplet pairing being present, but also $^{130}_{64}$Gd→ $^{132}_{64}$Gd is likely to occur, which coincides with spin-singlet pairing.

We are hopeful to see future experiments that can verify our predictions in this region of the nuclear chart. In addition, in a future work, the framework developed and tested here, will be applied to lighter isotopes, where mixed-spin pairing might be present, and which could be within reach of current experiments.

ACKNOWLEDGMENTS

The authors are thankful to G. F. Bertsch and D. Lacroix for insightful discussions. This work was supported in part by the Natural Sciences and Engineering Research Council (NSERC) of Canada, the Canada Foundation for Innovation (CFI), the Early Researcher Award (ERA) program of the Ontario Ministry of Research, Innovation and Science, the U.S. Department of Energy, Office of Science, Office of Nuclear Physics under Contracts DE-FG02-10ER41700 (FUSTIPEN) and DEAC02-05CH11231 (LBNL). Computational resources were provided by SHARCNET and NERSC.

---

[1] A. Bohr, B. R. Mottelson, and D. Pines, Phys. Rev. **110**, 936 (1958).
[2] D. J. Dean and M. Hjorth-Jensen, Rev. Mod. Phys. **75**, 607 (2003).
[3] D. Brink and R. Broglia, *Nuclear Superfluidity: Pairing in Finite Systems*, Cambridge Monographs on Particle Physics, Nuclear Physics and Cosmology (Cambridge University Press, 2010).
[4] R. Broglia and V. Zelevinsky, eds., *Fifty Years of Nuclear BCS* (World Scientific, 2013).
[5] S. Frauendorf and A. O. Macchiavelli, Prog. Part. Nucl. Phys. **78**, 24 (2014).
[6] V. G. J. Stoks, R. A. M. Klomp, M. C. M. Rentmeester, and J. J. de Swart, Phys. Rev. C **48**, 792 (1993).
[7] J. Engel, K. Langanke, and P. Vogel, Phys. Lett. B **389**, 211 (1996).
[8] J. Engel, L. K., and P. Vogel, Phys. Lett. B **429**, 215 (1998).
[9] K. Langanke, D. J. Dean, P. B. Radha, Y. Alhassid, and S. E. Koonin, Phys. Rev. C **52**, 718 (1995).
[10] K. Langanke, D. J. Dean, P. B. Radha, and S. E. Koonin, Nucl. Phys. **A602**, 244 (1996).
[11] K. Langanke, D. J. Dean, S. E. Koonin, and P. B. Radha, Nucl. Phys. **A613**, 253 (1997).
[12] K. Langanke, P. Vogel, and D. C. Zheng, Nucl. Phys. A **626**, 735 (1997).
[13] D. Dean, S. Koonin, K. Langanke, and P. Radha, Phys. Lett. B **399**, 1 (1997).
[14] A. Poves and G. Martinez-Pinedo, Phys. Lett. B **430**, 203 (1998).
[15] G. Martinez-Pinedo, K. Langanke, and P. Vogel, Nucl. Phys. **A651**, 379 (1999).
[16] A. Poves and G. Martinez-Pinedo, Phys. Lett. B **430**, 203 (1998).
[17] S. Baroni, A. O. Macchiavelli, and A. Schwenk, Phys. Rev. C **81**, 064308 (2010).
[18] D. Bonatsos, I. E. Assimakis, N. Minkov, A. Martinou, R. B. Cakirli, R. F. Casten, and K. Blaum, Phys. Rev. C **95**, 064325 (2017).
[19] P. Ring and P. Schuck, *The Nuclear Many Body Problem* (Springer-Verlag, New York, Heidelberg, Berlin, 1980).
[20] P. Camiz, A. Covello, and M. Jean, Il Nuovo Cimento (1955-1965) **36**, 663 (1965).
[21] P. Camiz, A. Covello, and M. Jean, Il Nuovo Cimento B (1965-1970) **42**, 199 (1966).
[22] J. N. Ginocchio and J. Weneser, Phys. Rev. **170**, 859 (1968).
[23] A. Goswami, Nucl. Phys. **60**, 228 (1964).
[24] A. Goswami and L. S. Kisslinger, Phys. Rev. **140**, B26 (1965).
[25] H. C. Chen and A. Goswami, Phys. Lett. B **24**, 257 (1967).
[26] A. Goodman, G. Struble, and A. Goswami, Phys. Lett. B **26**, 260 (1968).
[27] H. H. Wolter, A. Faessler, and P. Sauer, Phys. Lett. B **31**, 516 (1970).
[28] H. H. Wolter, A. Faessler, and P. Sauer, Nucl. Phys. A **167**, 108 (1971)
.
[29] A. Gezerlis, G. F. Bertsch, and Y. L. Luo, Phys. Rev. Lett. **106**, 252502 (2011).
[30] B. Bulthuis and A. Gezerlis, Phys. Rev. C **93**, 014312 (2016).
[31] G. F. Bertsch and Y. Luo, Phys. Rev. C **81**, 064320 (2010).
[32] L. M. Robledo and G. F. Bertsch, Phys. Rev. C **84**, 014312 (2011).
[33] N. Onishi and S. Yoshida, Nucl. Phys. **80**, 367 (1966).
[34] K. Neergård and E. Wüst, Nucl. Phys. A **402**, 311 (1983).
[35] Q. Haider and D. Gogny, J. Phys. G **18**, 993 (1992).
[36] F. Dönau, Phys. Rev. C **58**, 872 (1998).
[37] L. M. Robledo, Phys. Rev. C **79**, 021302 (2009).
[38] G. F. Bertsch and L. M. Robledo, Phys. Rev. Lett. **108**, 042505 (2012).
[39] B. Avez and M. Bender, Phys. Rev. C **85**, 034325 (2012).
[40] O. Makito and T. Mizusaki, Phys. Lett. B **707**, 305 (2012).
[41] M. Grasso, D. Lacroix, and A. Vitturi, Phys. Rev. C **85**, 034317 (2012).
[42] L. M. Robledo, Phys. Rev. C **84**, 014307 (2011).
[43] H. Georgi, *Lie Algebras in Particle Physics* (Sarat Book Distributors, 2009).
[44] J. Ripoche, D. Lacroix, D. Gambacurta, J.-P. Ebran, and T. Duguet, Phys. Rev. C **95**, 014326 (2017).
[45] D. Lacroix and D. Gambacurta, Phys. Rev. C **86**, 014306 (2012).
[46] M. Wimmer, ACM Trans. Math. Softw. **38** (2012).
[47] A. R. Edmonds, *Angular momentum in quantum mechanics* (Princeton University Press, Princeton, New Jersey, 1957).
[48] H. Shimoyama and M. Matsuo, Phys. Rev. C **84**, 044317 (2011).
[49] Y. Tanimura, H. Sagawa, and K. Hagino, Prog. Theo. Exp. Phys. **2014**, 053D02 (2014).
[50] G. H. Golub and C. F. Van Loan, *Matrix Computations (3rd Ed.)* (Johns Hopkins University Press, Baltimore, MD, USA, 1996).
[51] H. V. Henderson and S. R. Searle, Linear and Multilinear Algebra **9**, 271 (1981).